ROCK PHYSICS 3

Quantitative Facies Interpretation

Kyle Spikes

Facies identification from well data and mapping to seismic data

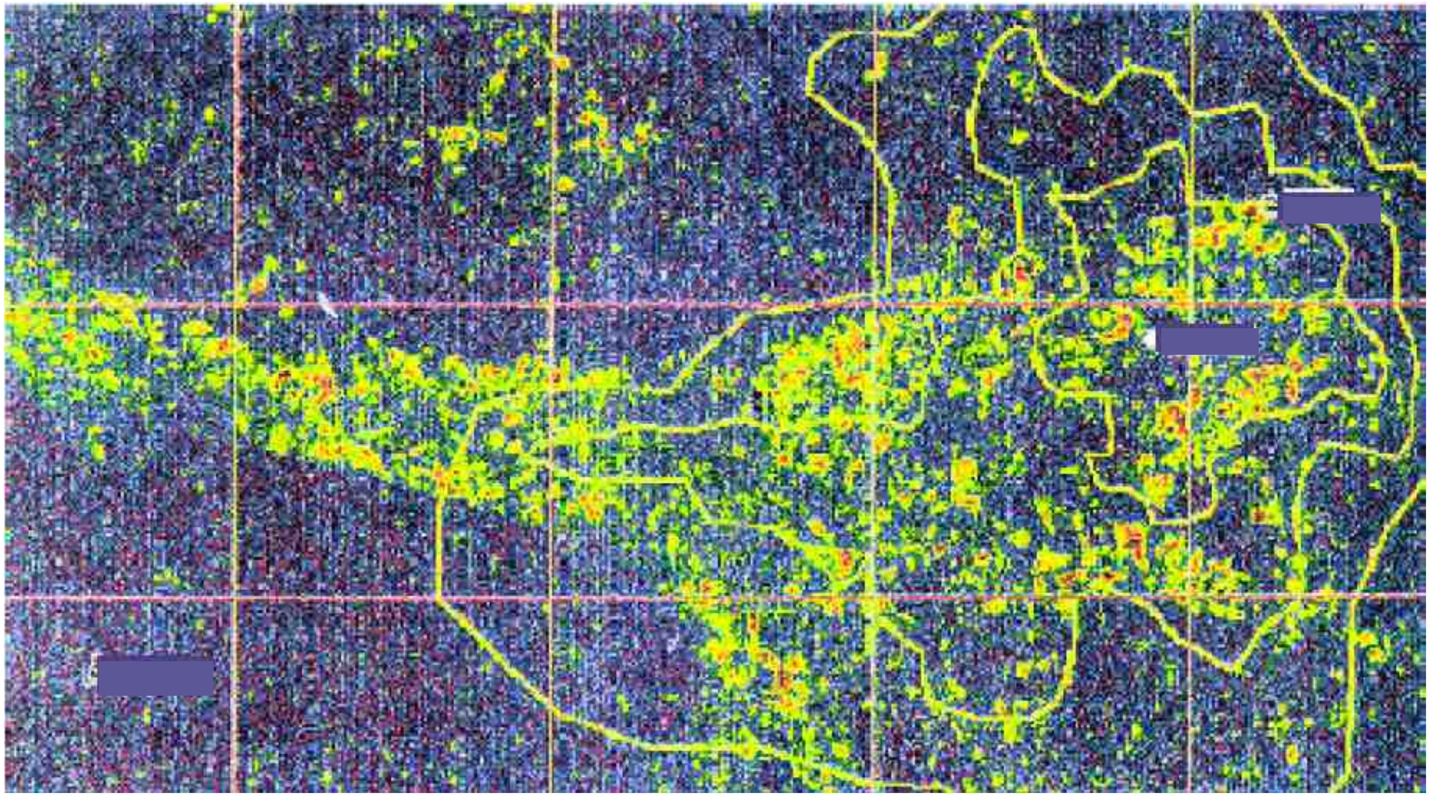

From Avseth et al., 2005

What controls the amplitude?
Lithology, porosity, pore fluids, stresses
… but also sedimentation and diagenesis

Top Heimdal in the North Sea

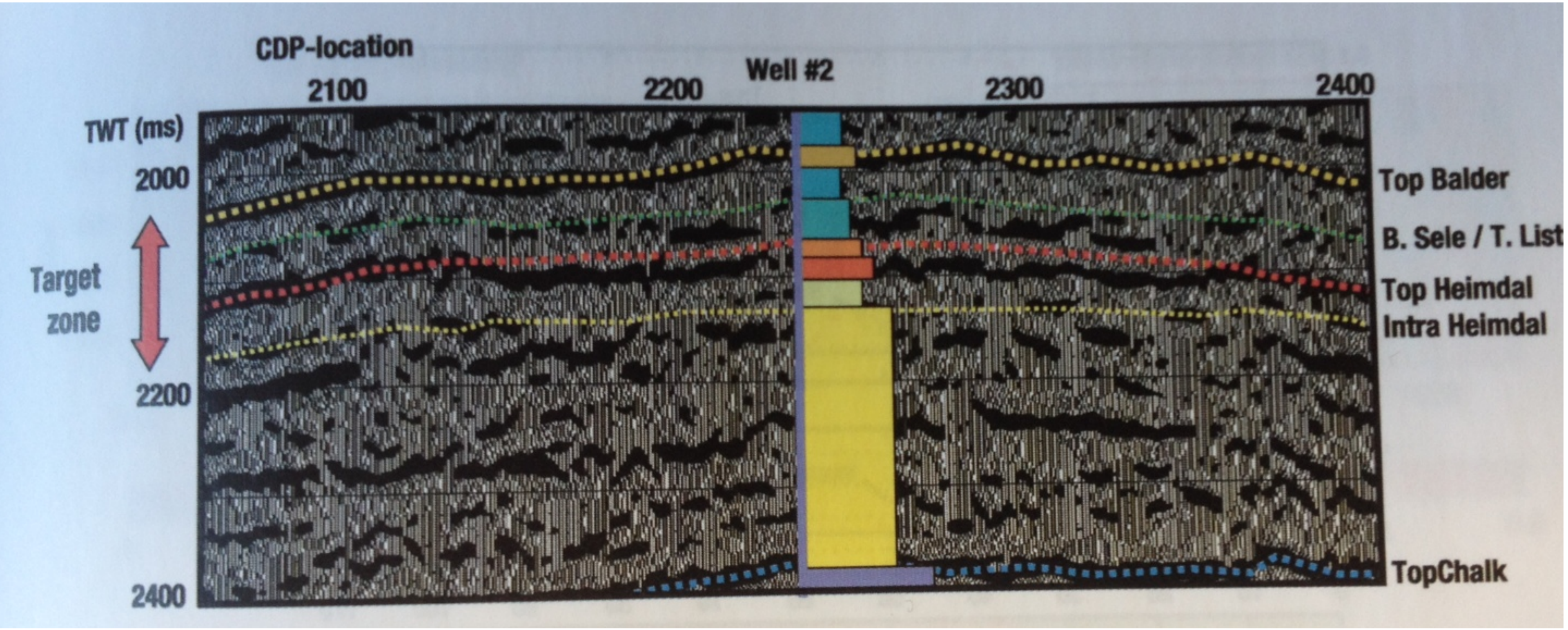

From Avseth et al., 2005

Type well and facies

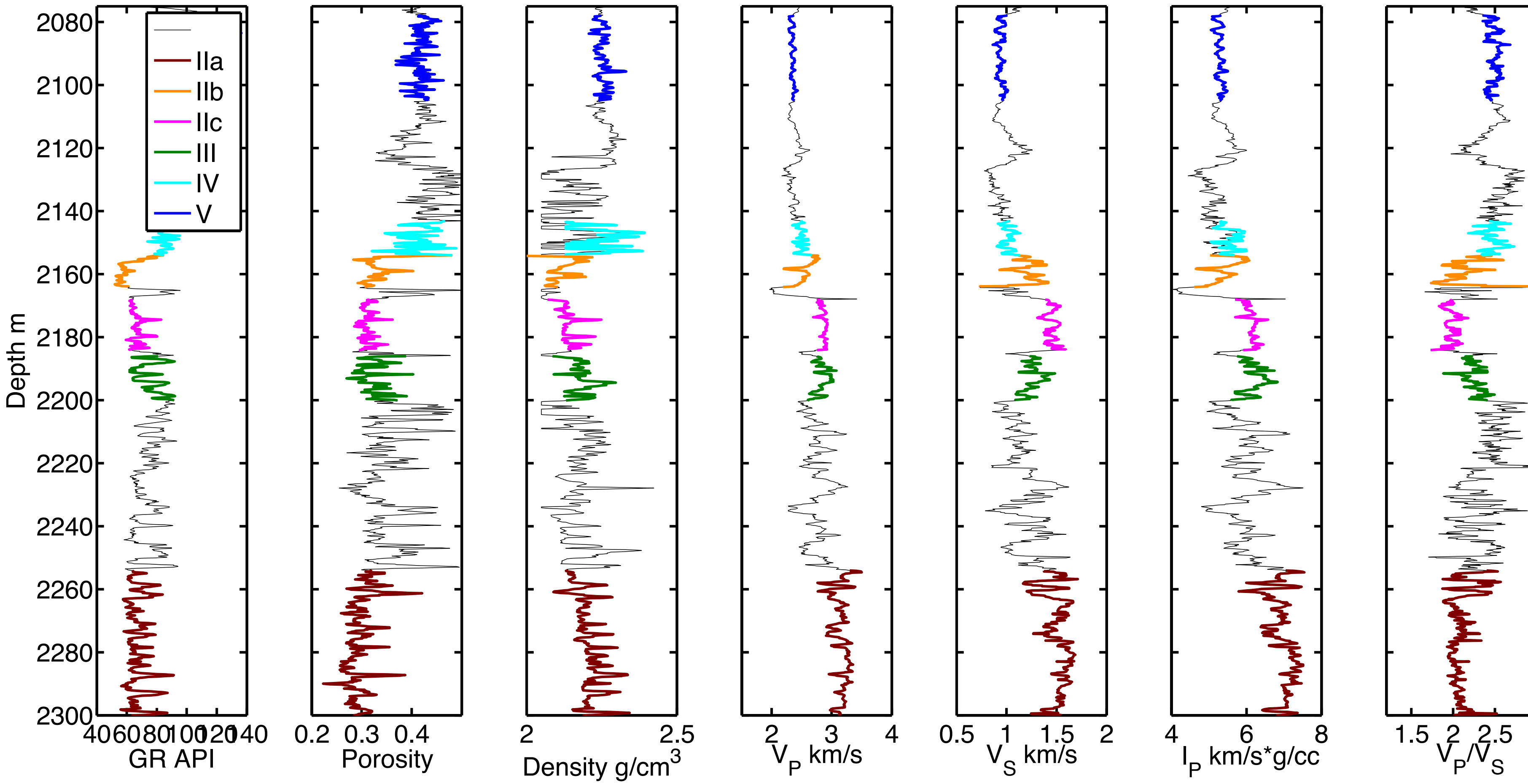

IIa = Cemented Sandstone
IIb = Clean Sandstone 1
IIc = Clean Sandstone 2

III = Shaley Sandstone
IV = Silty Shale
V = Shale

Type well and facies

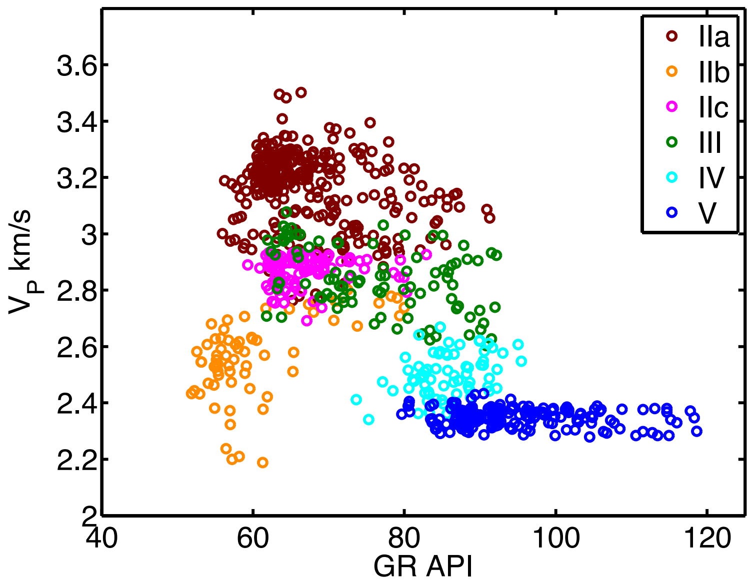

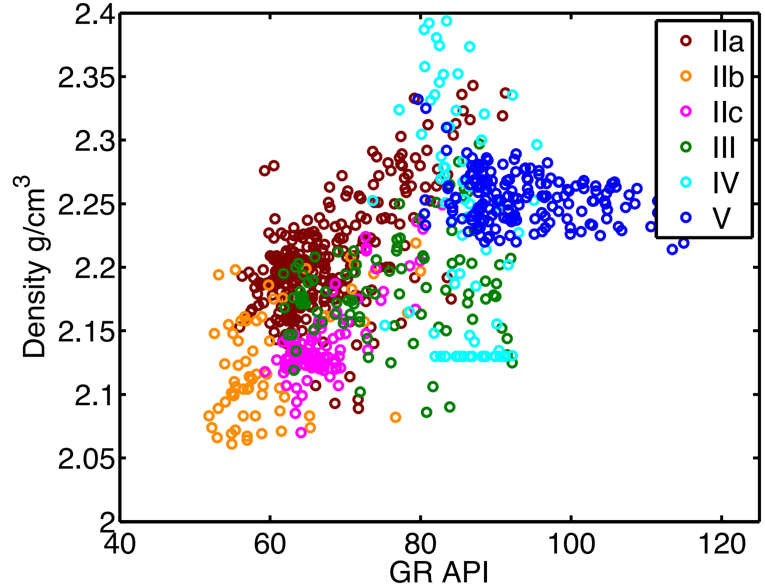

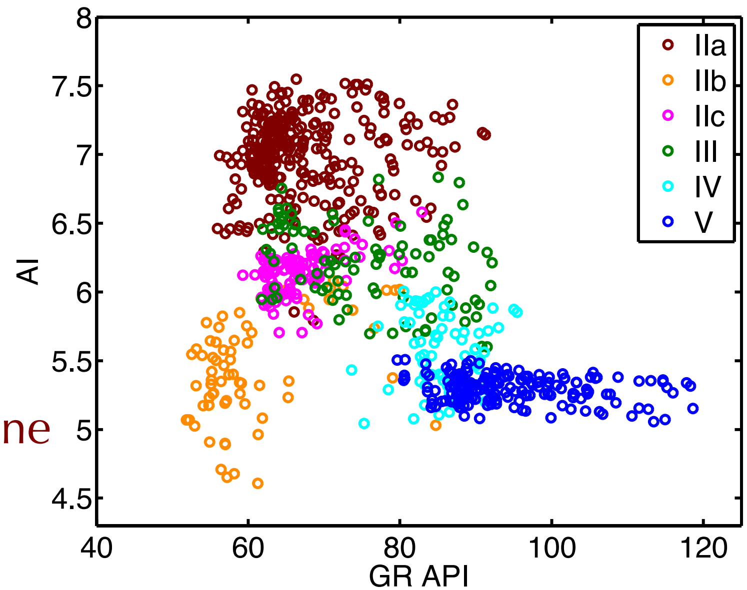

IIa = Cemented Sandstone
IIb = Clean Sandstone 1
IIc = Clean Sandstone 2

III = Shaley Sandstone
IV = Silty Shale
V = Shale

Type well and facies

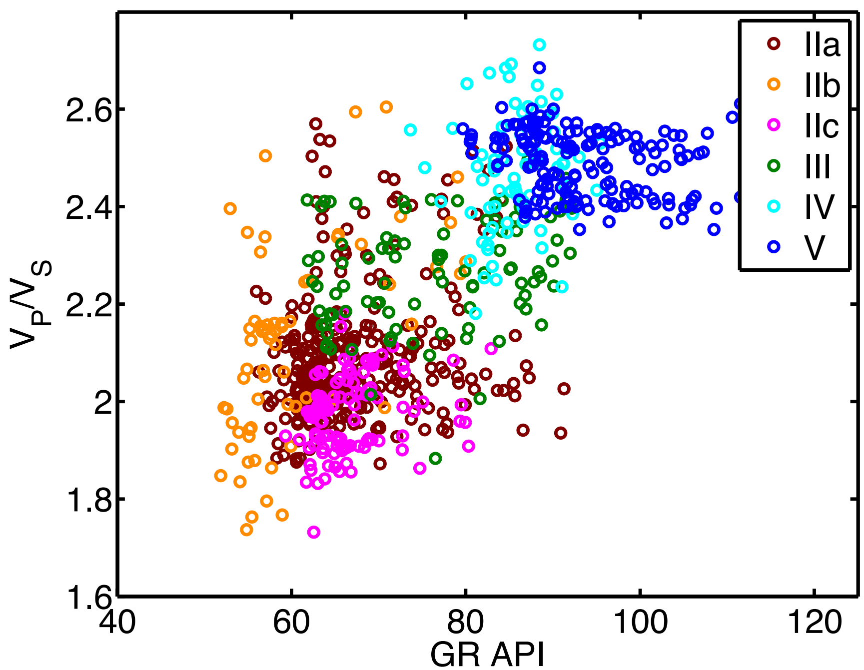

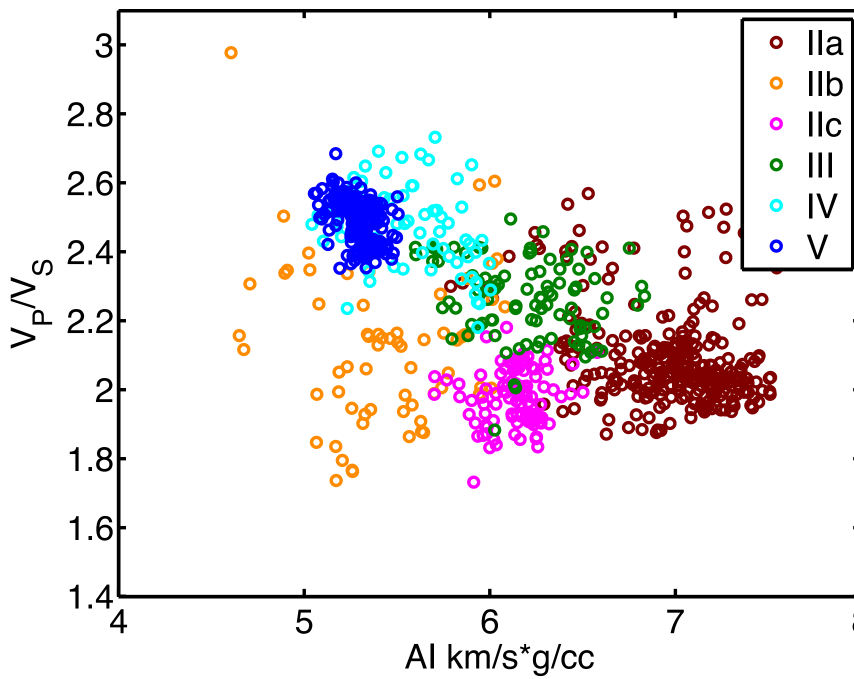

IIa = Cemented Sandstone
IIb = Clean Sandstone 1
IIc = Clean Sandstone 2

III = Shaley Sandstone
IV = Silty Shale
V = Shale

Overview

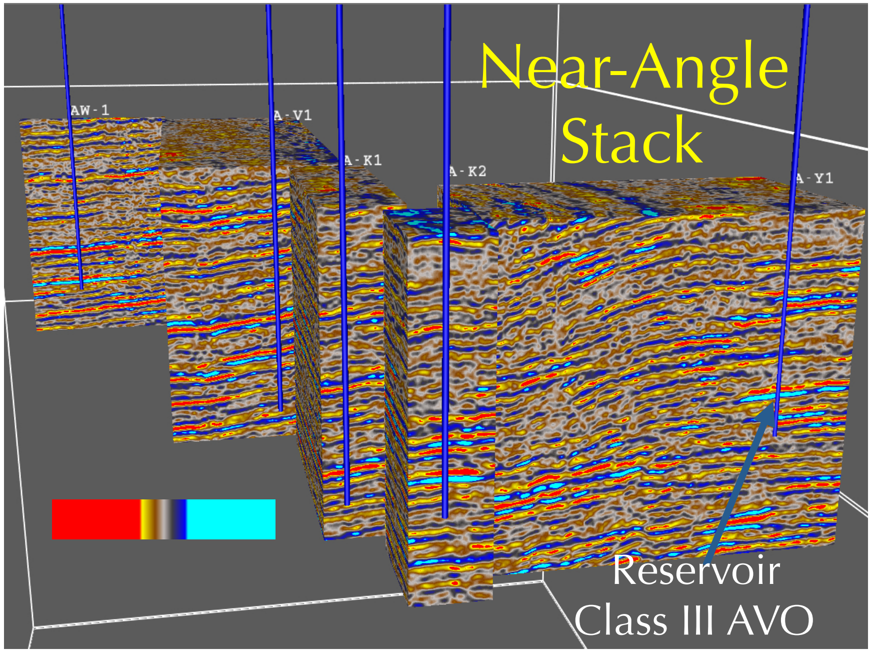

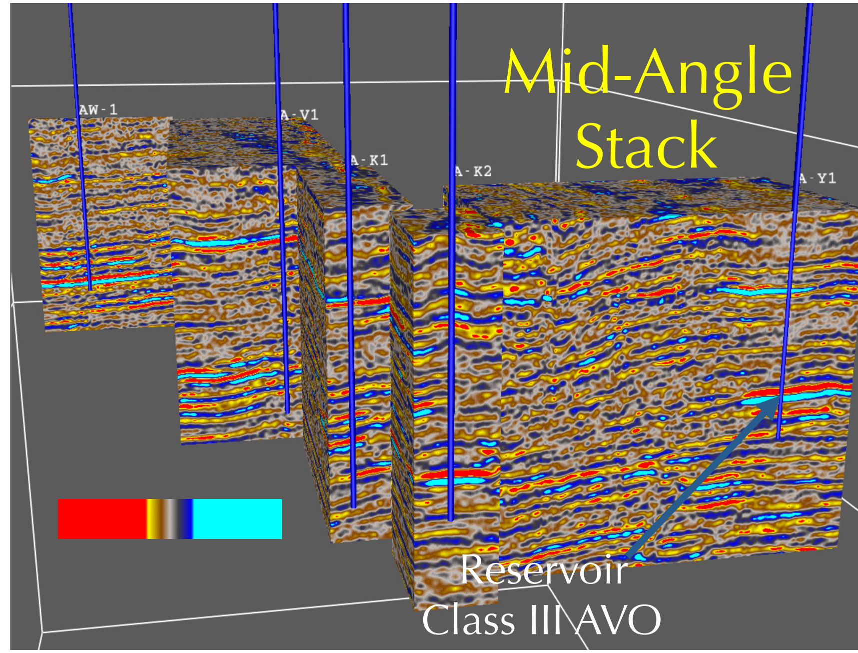

CDP Gather

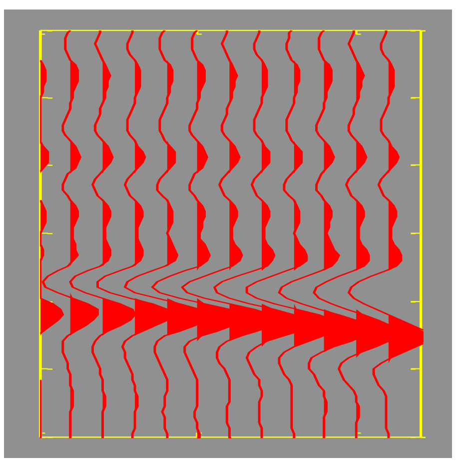

Geologic interpretation

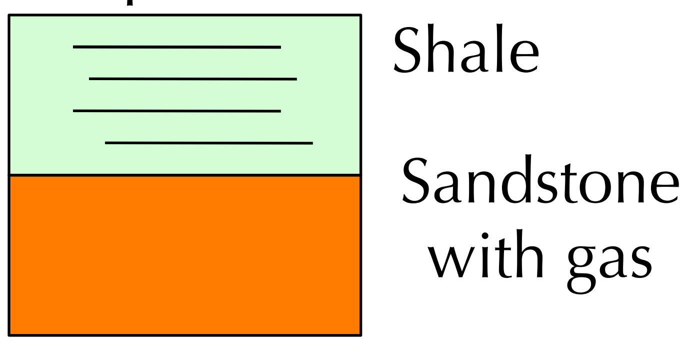

AVO response at reservoir

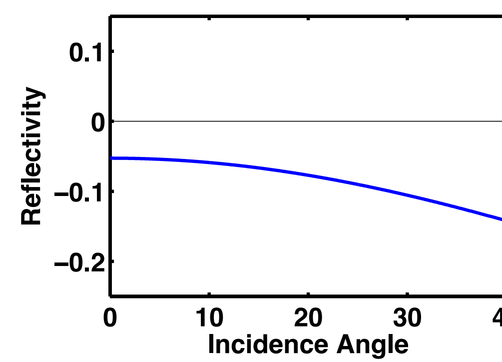

AVO Attributes
Intercept and Gradient

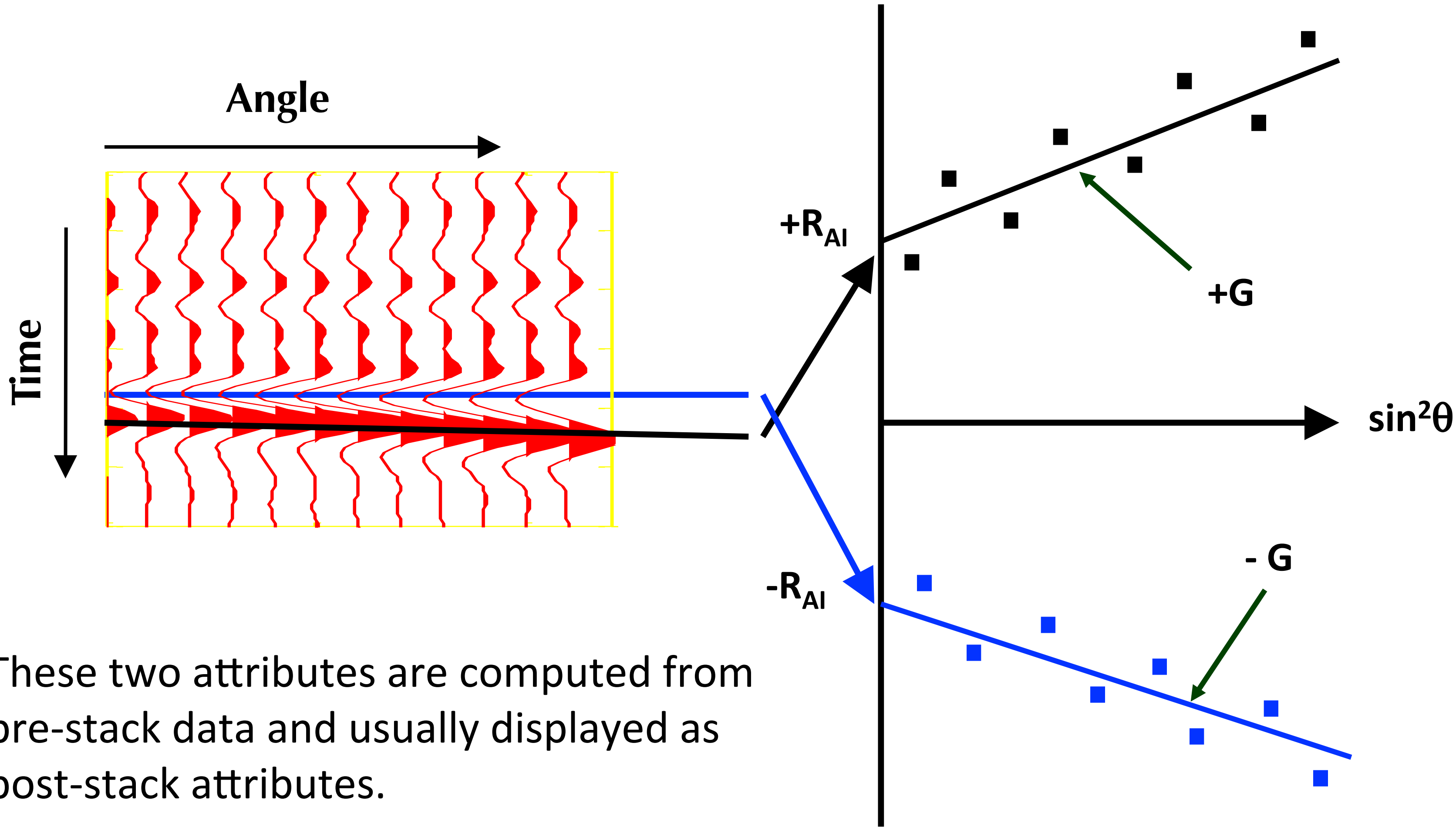

These two attributes are computed from pre-stack data and usually displayed as post-stack attributes.

The reflection coefficient

In an isotropic medium:

A wave that is incident on a boundary will generally result in two reflected waves (one P and one S) and two transmitted waves.

The angles of incidence and transmission are a function of Snell's law, written here in general for any of the waves and angles.

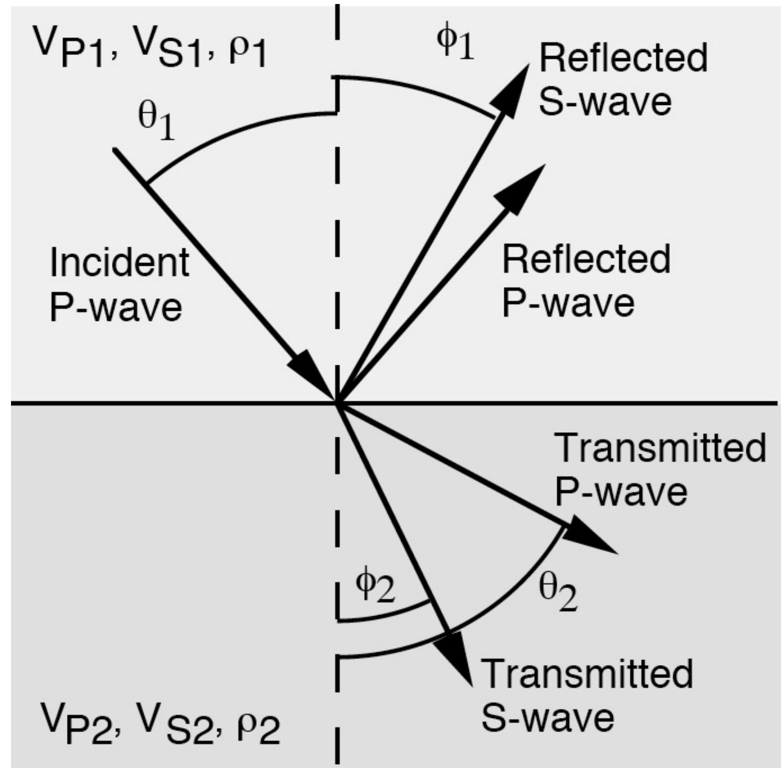

$$\frac{\sin\theta_1}{V_{P1}} = \frac{\sin\theta_2}{V_{P2}} = \frac{\sin\phi_1}{V_{S1}} = \frac{\sin\phi_2}{V_{S2}}$$

Examples of angle-dependent reflectivity

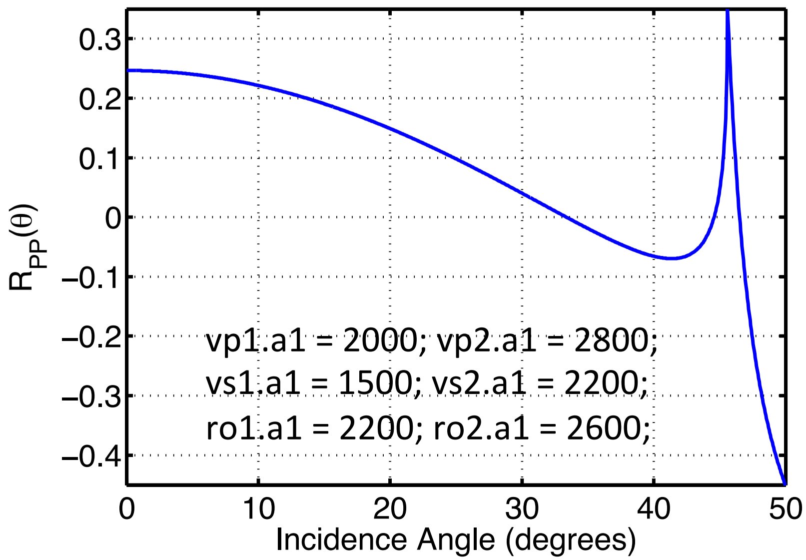

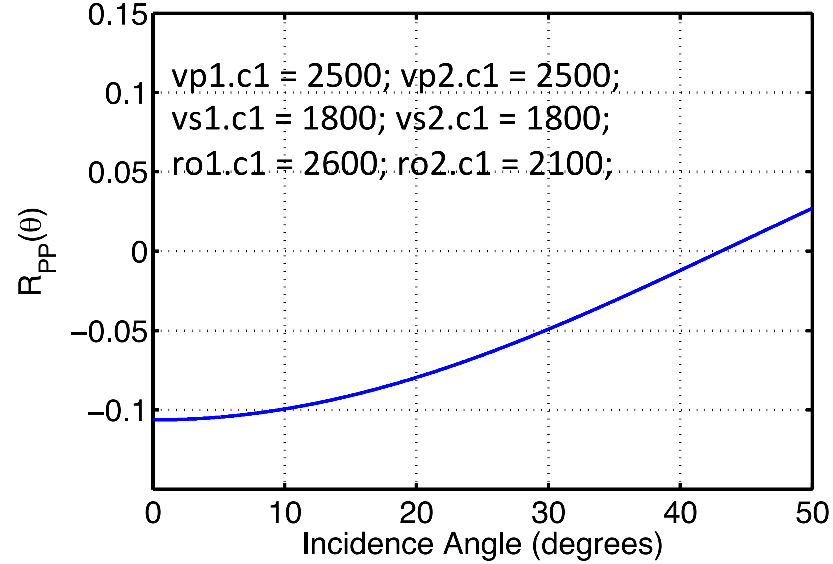

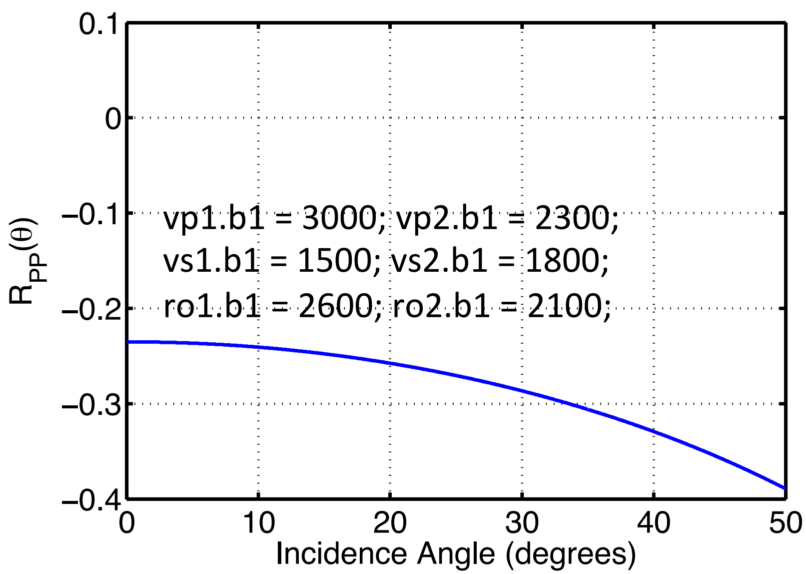

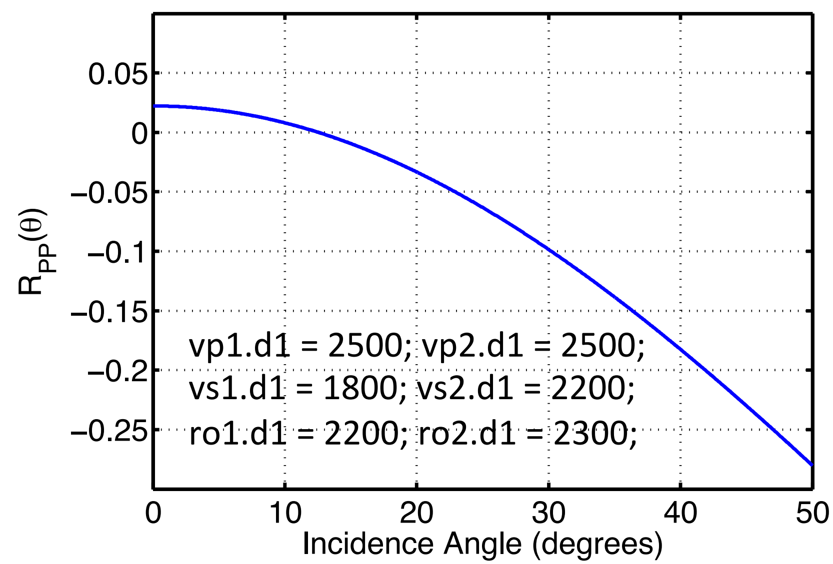

AVO – Full Zoeppritz vs. approximations

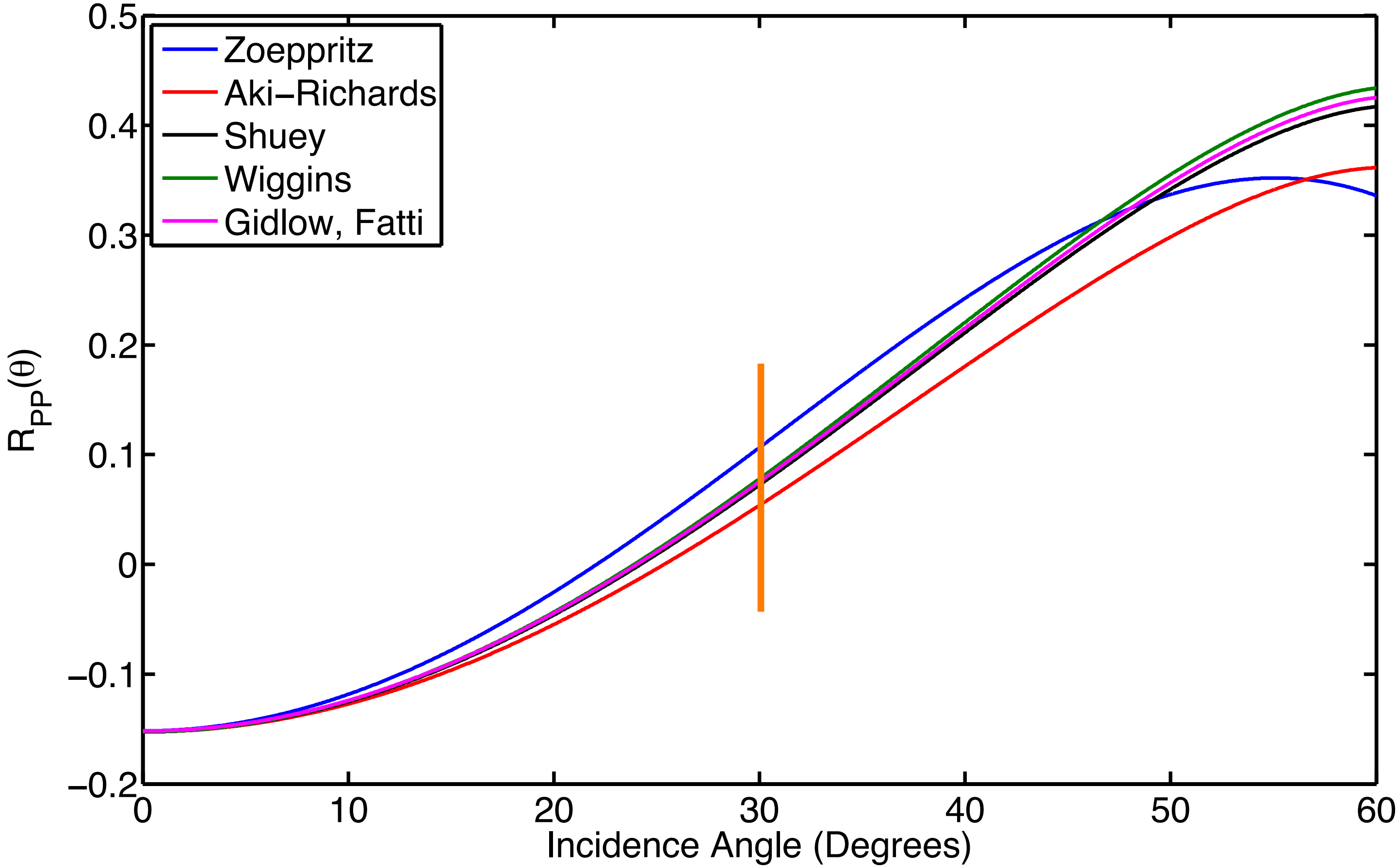

The angle limit for the approximations is typically take at about 30 degrees. This can vary depending on the rock property contrasts.

Wide-aperture (long-offset) seismic data is prone to the effects of post-critical reflections (beyond the critical angle. Thus, any AVO interpretation must consider this and not push to extremely large angles.

Synthetic seismic data examples
2D Prestack CMP Gather

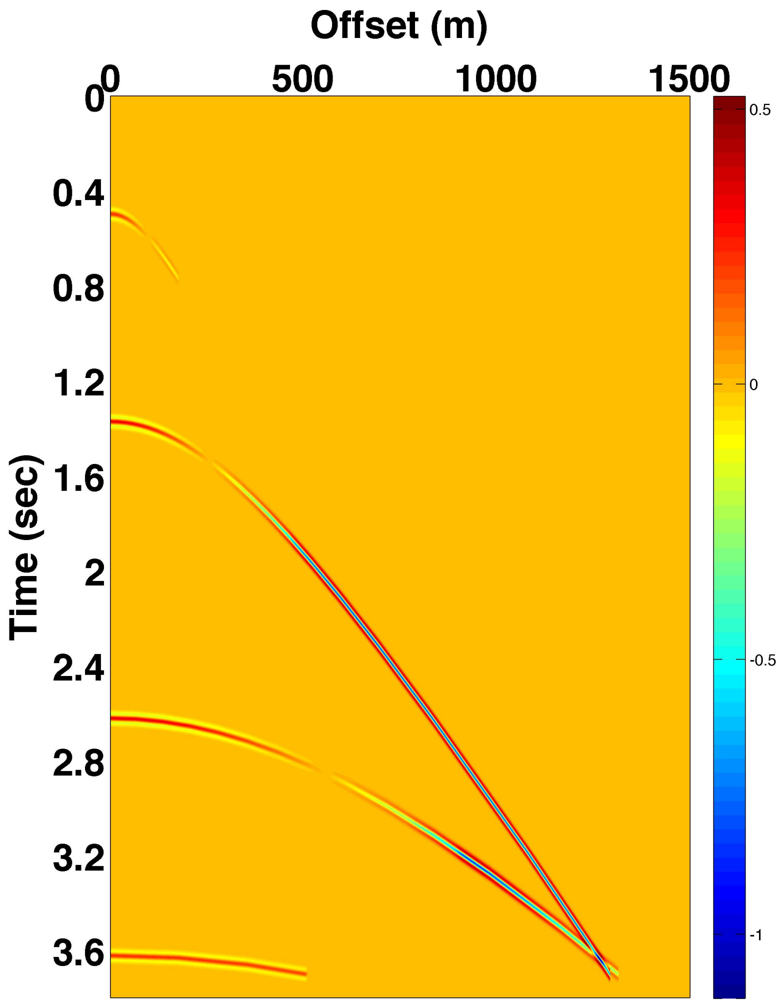

CMP Gather

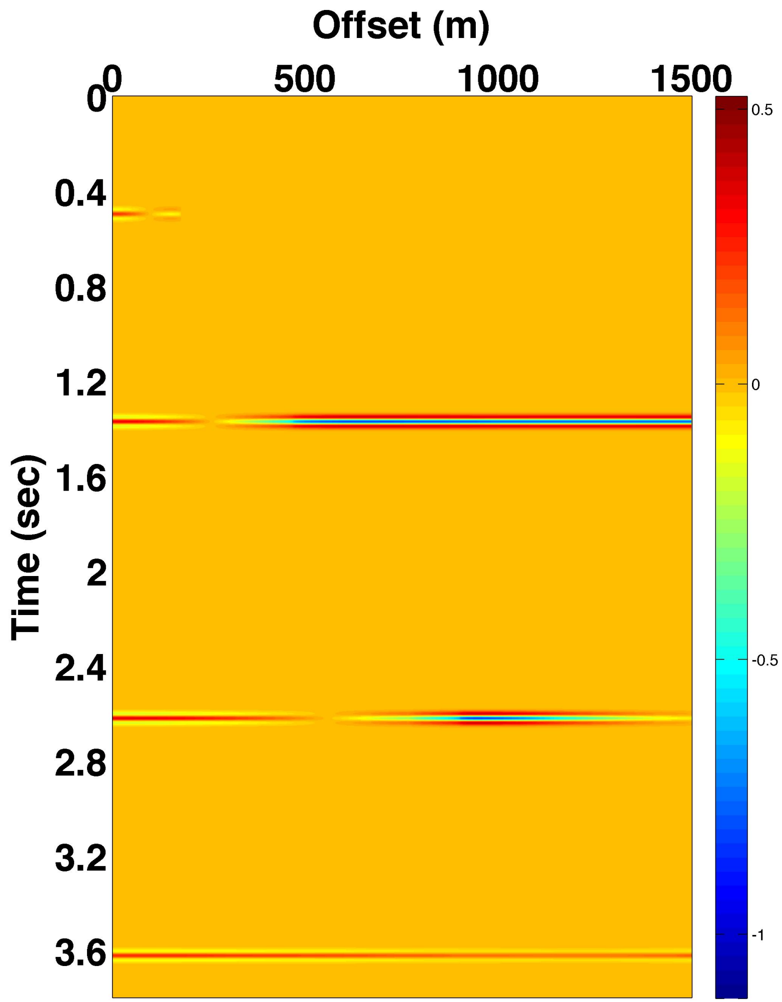

Normal moveout (NMO) corrected CMP Gather

AVO - Shuey's Approximation

A further approximation of Aki-Richards

$$R(\theta) \approx R_0 + G\sin^2\theta + F\left[\tan^2\theta - \sin^2\theta\right]$$

$$R_0 = R(0) \approx \frac{1}{2}\left(\frac{\Delta V_P}{V_P} + \frac{\Delta\rho}{\rho}\right)$$

$$G = \frac{1}{2}\frac{\Delta V_P}{V_P} - 2\frac{V_S^2}{V_P^2}\left(\frac{\Delta\rho}{\rho} + 2\frac{\Delta V_S}{V_S}\right)$$

$$G = R(0) - \frac{\Delta\rho}{\rho}\left(\frac{1}{2} + 2\frac{V_S^2}{V_P^2}\right) - 4\frac{V_S^2}{V_P^2}\frac{\Delta V_S}{V_S}$$

$$F = \frac{1}{2}\frac{\Delta V_P}{V_P}$$

This form can be interpreted in terms of different angular ranges.

R(0) is the normal-incidence reflection Coefficient

G is the gradient and describes the variation in the intermediate offsets

F dominates the far offsets near the critical angle.

For incidence angle less than about 30°, this can be reduced to:

$$R(\theta) \approx R_0 + G\sin^2\theta$$

$$\approx R(0) + G\sin^2\theta$$

AVO Attributes
Intercept and Gradient

Amplitudes are extracted at a given time, two of which are shown:

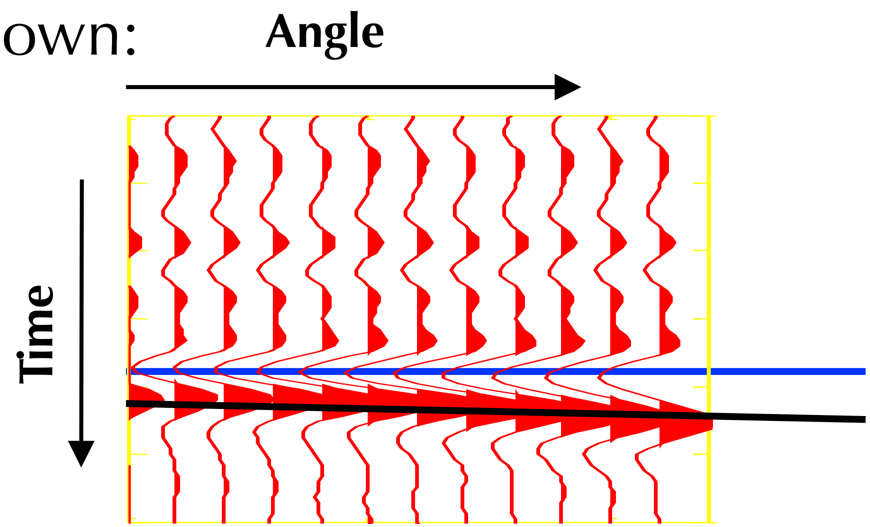

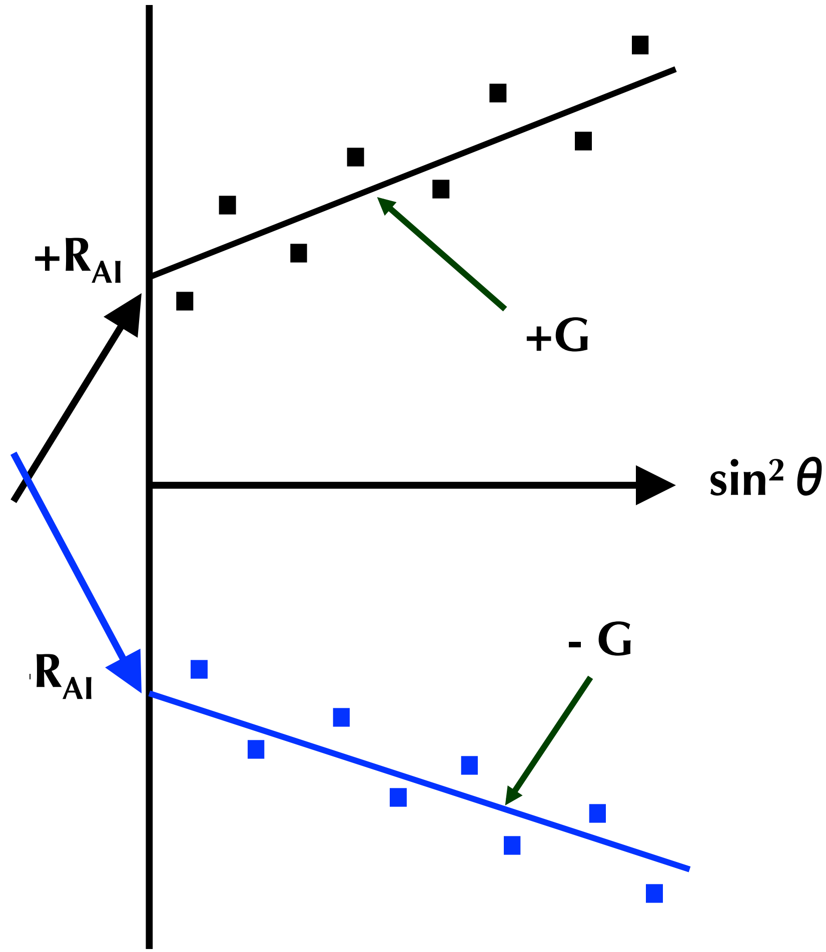

The Shuey equation predicts a linear relationship between these amplitudes and $\sin^2 \theta$. Regression curves are calculated to give $R(0)$ and G values for each time sample.

Estimating Intercept and Gradient

$$R(t,x) = R(t,0) + G(t)\sin^2\theta(t,x)$$

For a stratified Earth, the approximate relationship between offset (x) and incidence angle (θ) is

$$\sin^2\theta(t,x) \approx \frac{x}{(t_0^2 + x^2 / V_{RMS}^2)^{1/2}} \frac{V_{INT}}{V_{RMS}^2}$$

$$V_{RMS} = \text{RMS Velocity}$$
$$V_{INT} = \text{Interval Velocity}$$

For any two-way travel time at zero offset (t_0), R is measured at N offsets.

$$\begin{bmatrix} R(x_1) \\ R(x_2) \\ . \\ . \\ . \\ . \\ R(x_N) \end{bmatrix} = \begin{bmatrix} 1 & \sin^2\theta(t,x_1) \\ 1 & \sin^2\theta(t,x2) \\ & . \\ & . \\ & . \\ & . \\ 1 & \sin^2\theta(t,x_N) \end{bmatrix} \begin{bmatrix} R(t,0) \\ G(t) \end{bmatrix}$$

$$\mathbf{b = Ac}$$

$$\mathbf{c = (A^T A)^{-1}(A^T b)}$$

Intercept and Gradient for Top Heimdal

Compute the intercept and gradient terms at every sample at every CDP.

These images are the intercept and gradient values at the Top Heimdal

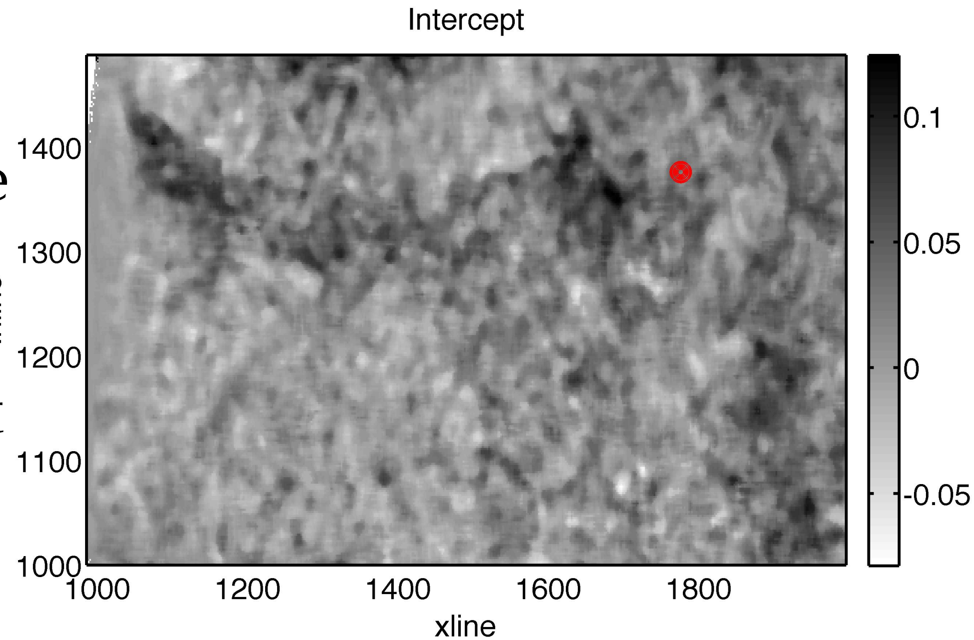

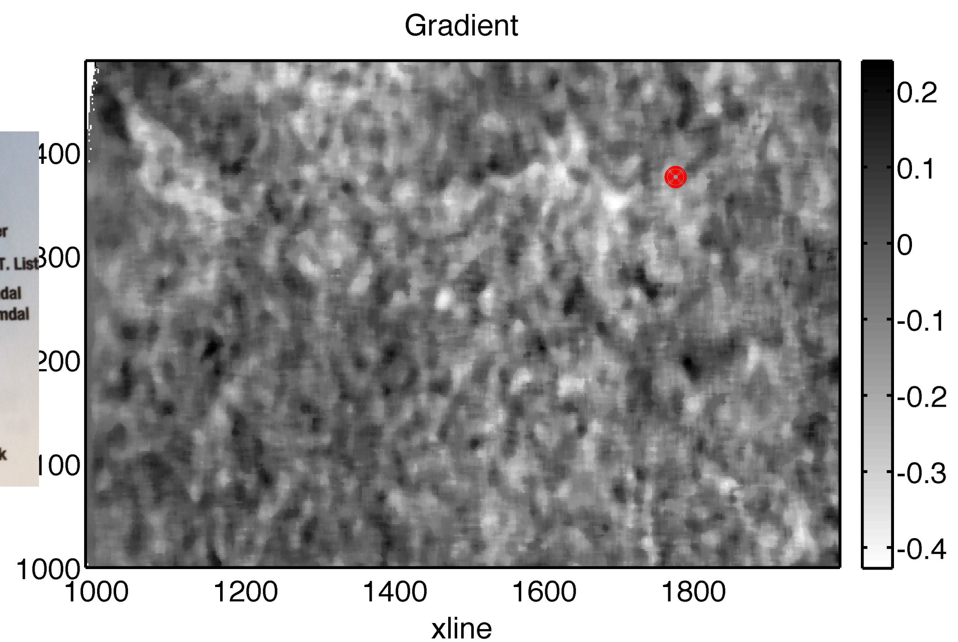

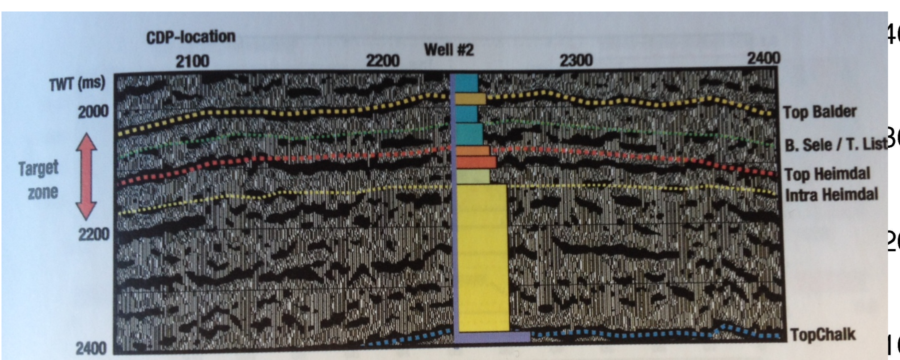

Intercept and Gradient for Top Heimdal

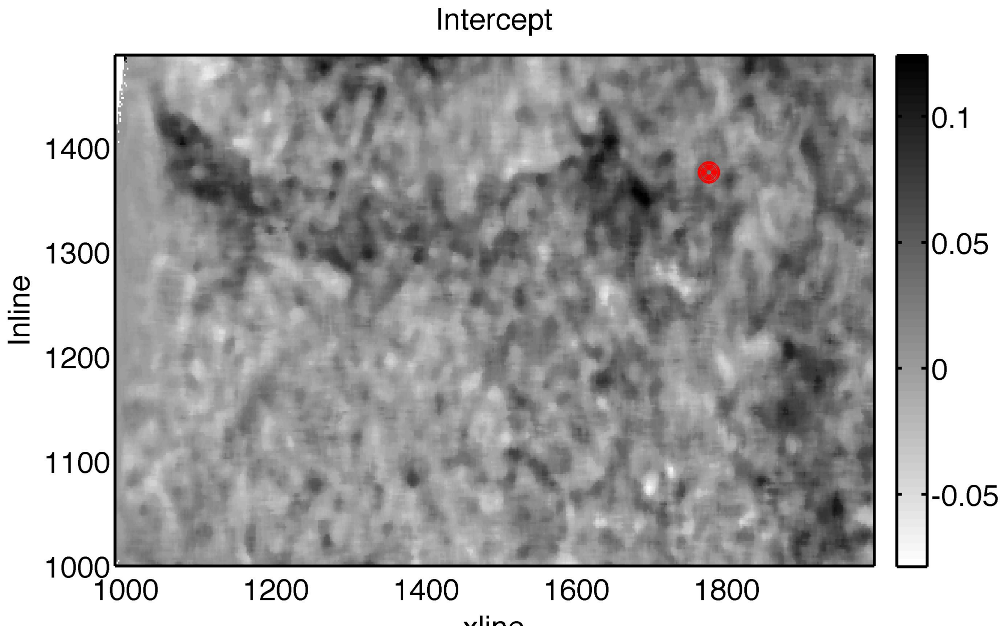

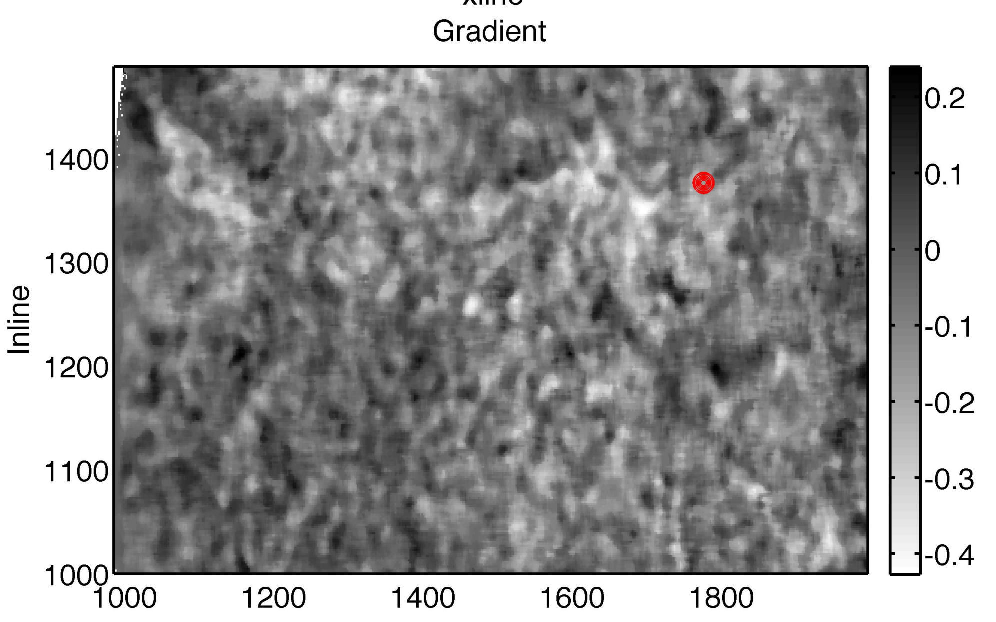

How do we relate the well-based facies to the seismic intercept and gradient data?

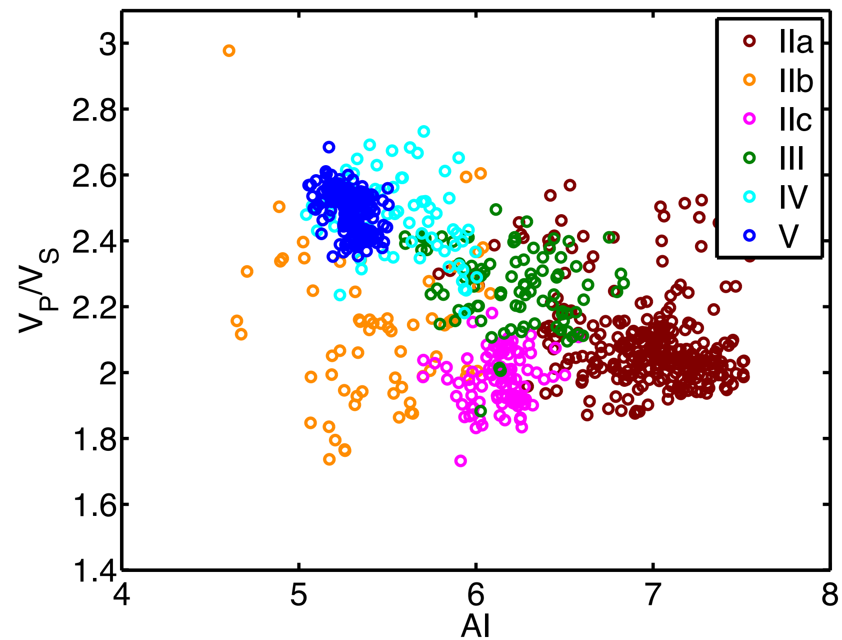

How do we relate the well-based facies to the seismic data?

Use the well-log facies information to compute distributions of synthetic intercept and gradient values

Step 1: Calculate PDFs and CDFs of each facies.

Step 2: Draw a given number of Monte-Carlo realizations from each PDF

Step 3: Compute Vp, Vs, density for different fluid saturations.

Step 4: Compute synthetic angle-dependent reflectivity for realizations of Facies IV overlying all the facies.

Step 5: Compute intercept and and gradient values for each reflectivity curve

Step 6: Use the Mahalanobis Distance to determine the most likely facies for the real intercept and gradient data.

Step 1: Calculate PDFs and CDFs of each facies

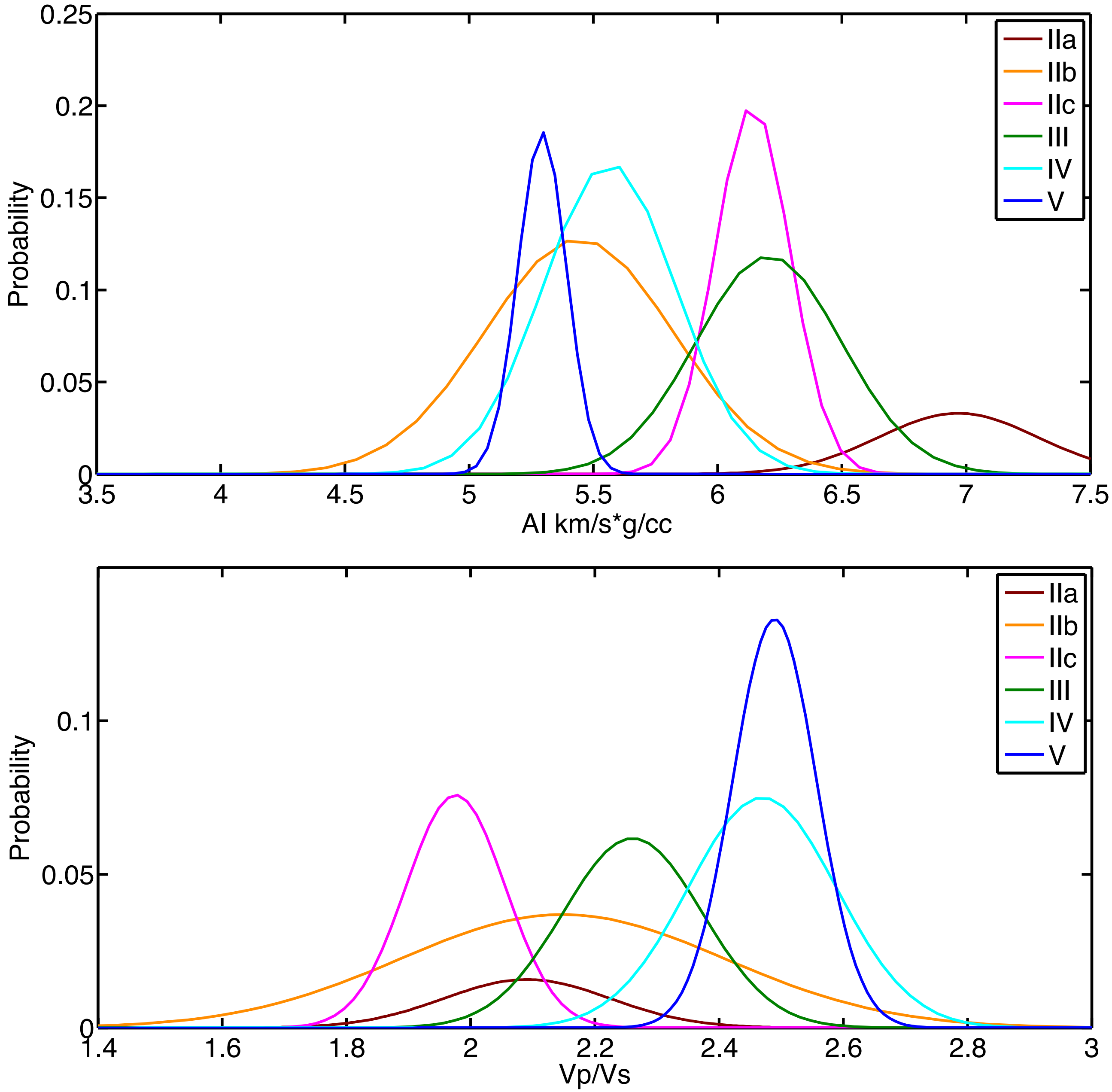

Step 1: Calculate PDFs and CDFs of each facies

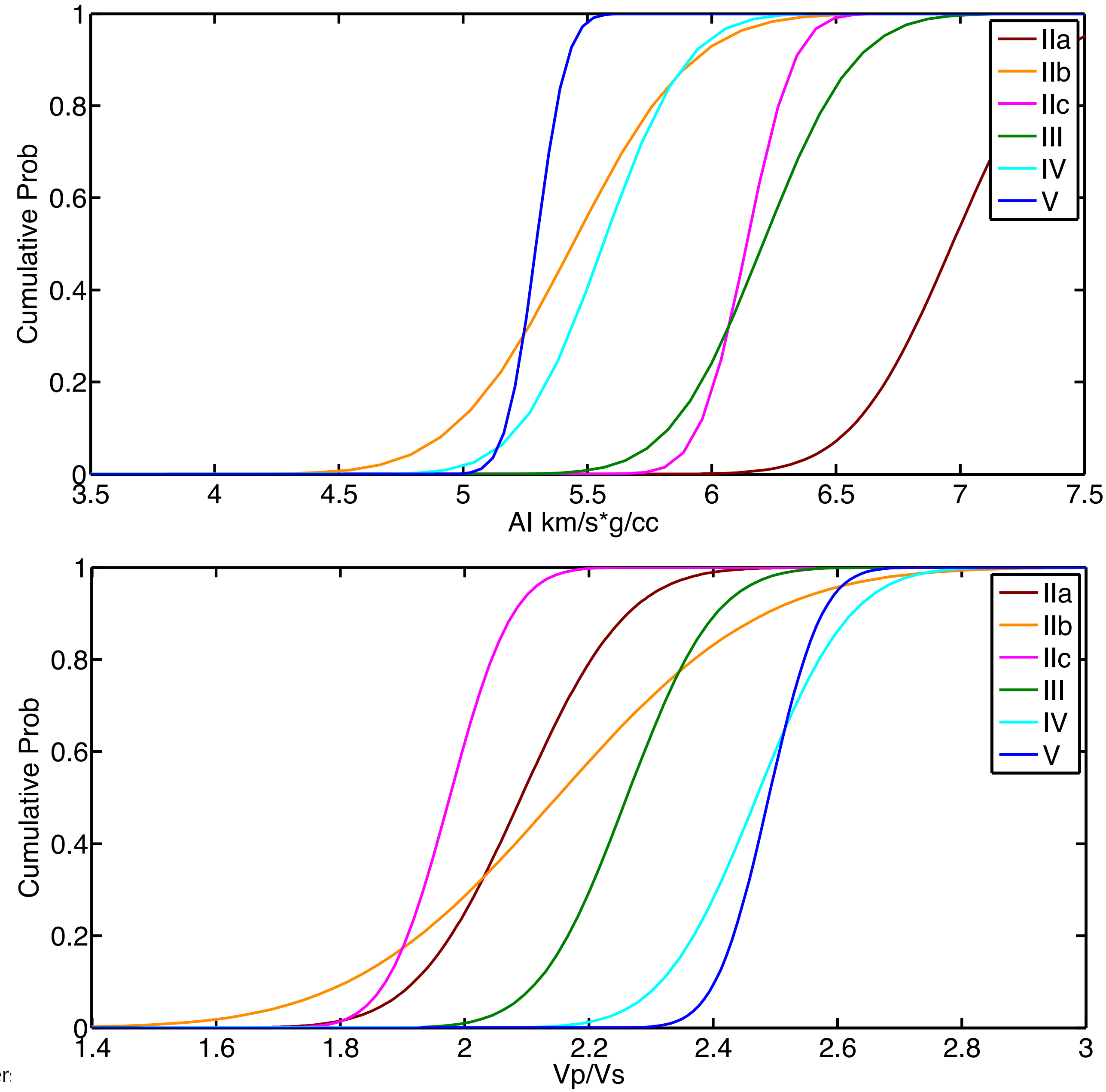

Step 2: Draw Monte-Carlo simulations

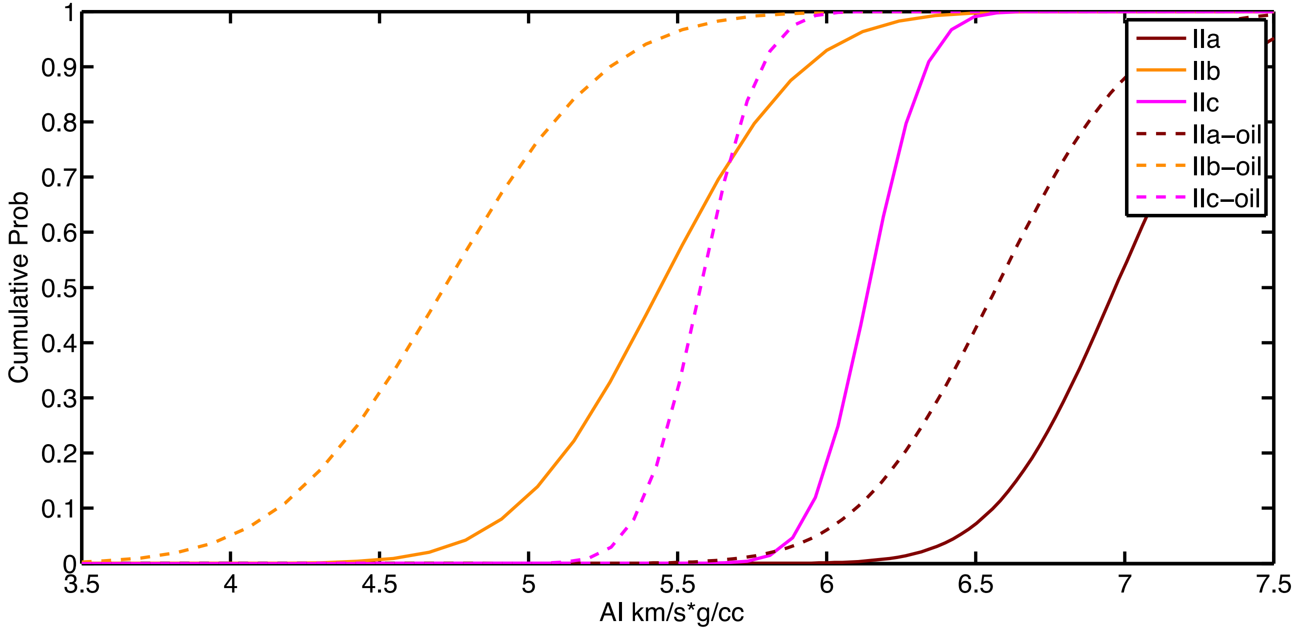

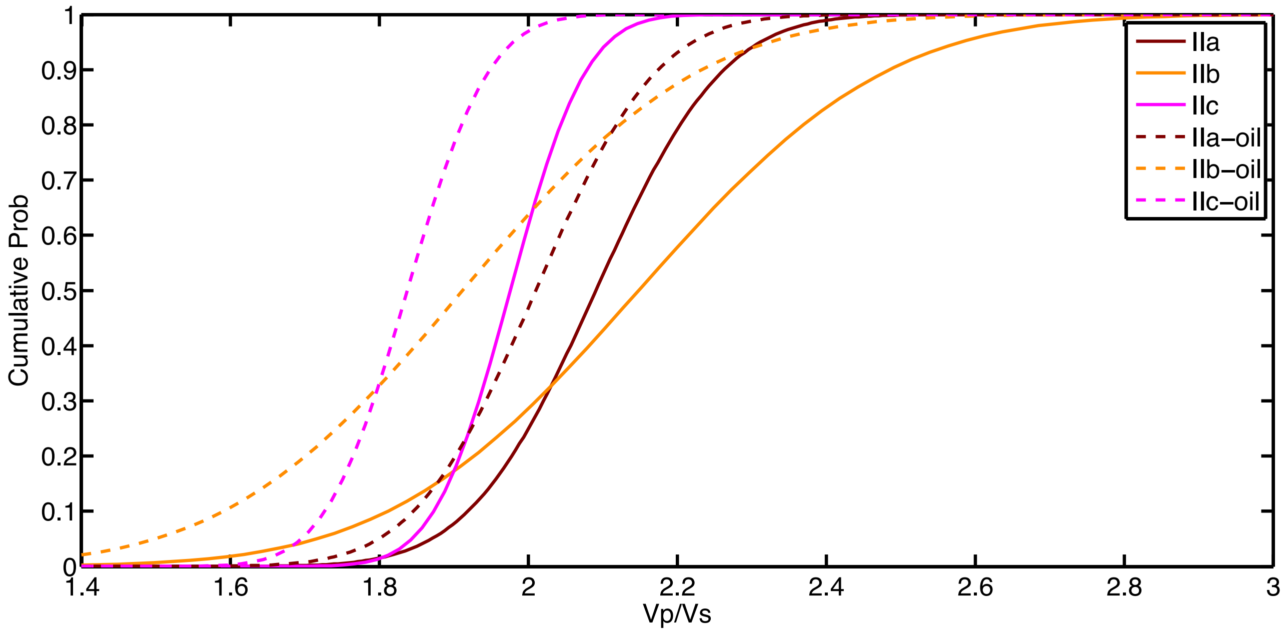

Step 3: Compute Vp, Vs, density for different fluids

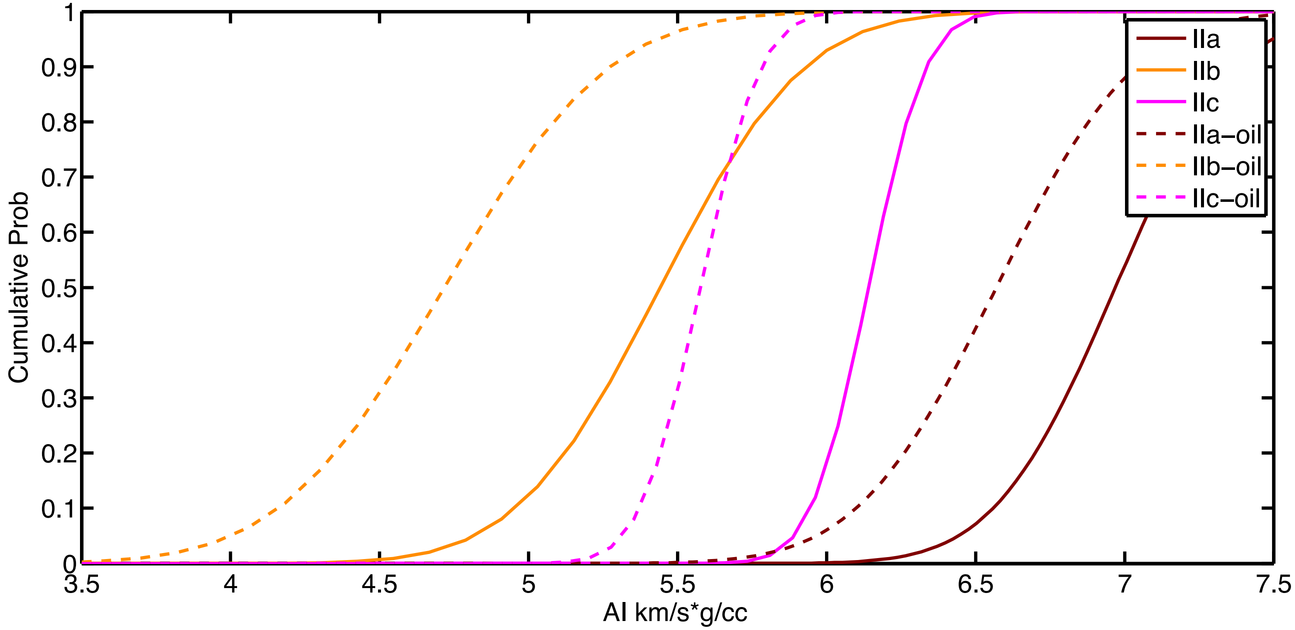

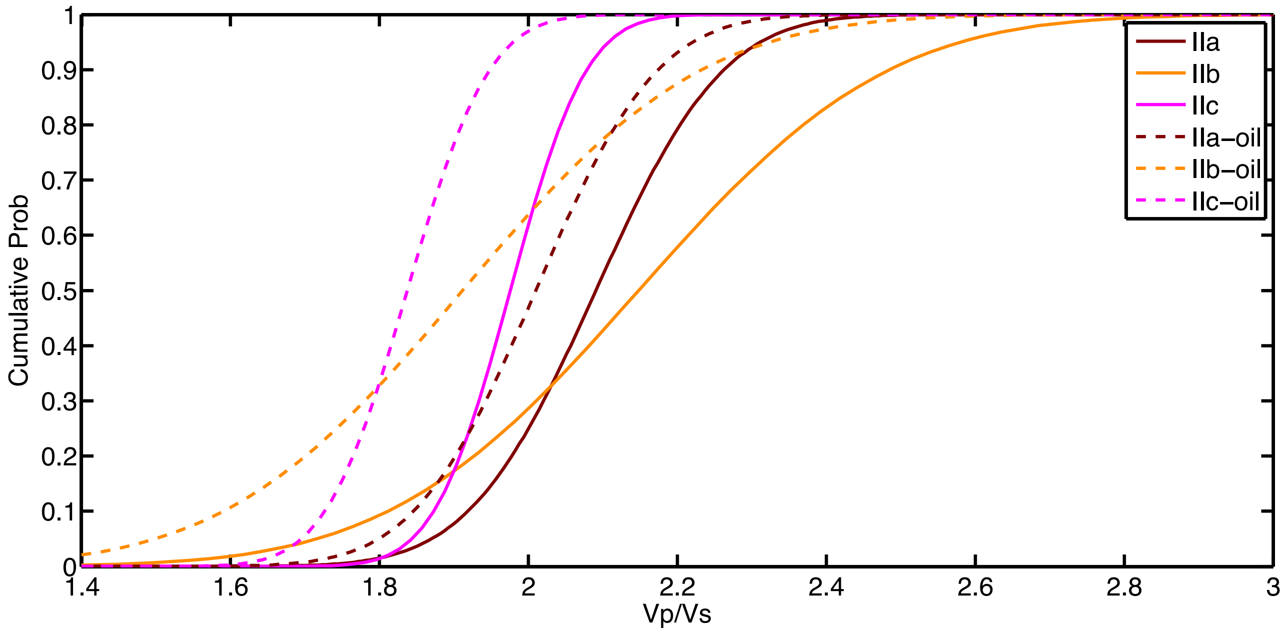

Step 4: Compute synthetic angle-dependent reflectivity for realizations of Facies IV overlying all the facies

Facies IV / Facies IIa-Oil	Facies IV / Facies IIb-Oil	Facies IV / Facies IIc-Oil
Facies IV / Facies IIa	Facies IV / Facies IIb	Facies IV / Facies IIc
Facies IV / Facies III	Facies IV / Facies IV	Facies IV / Facies V

Step 4: Compute synthetic angle-dependent reflectivity for realizations of Facies IV overlying all the facies

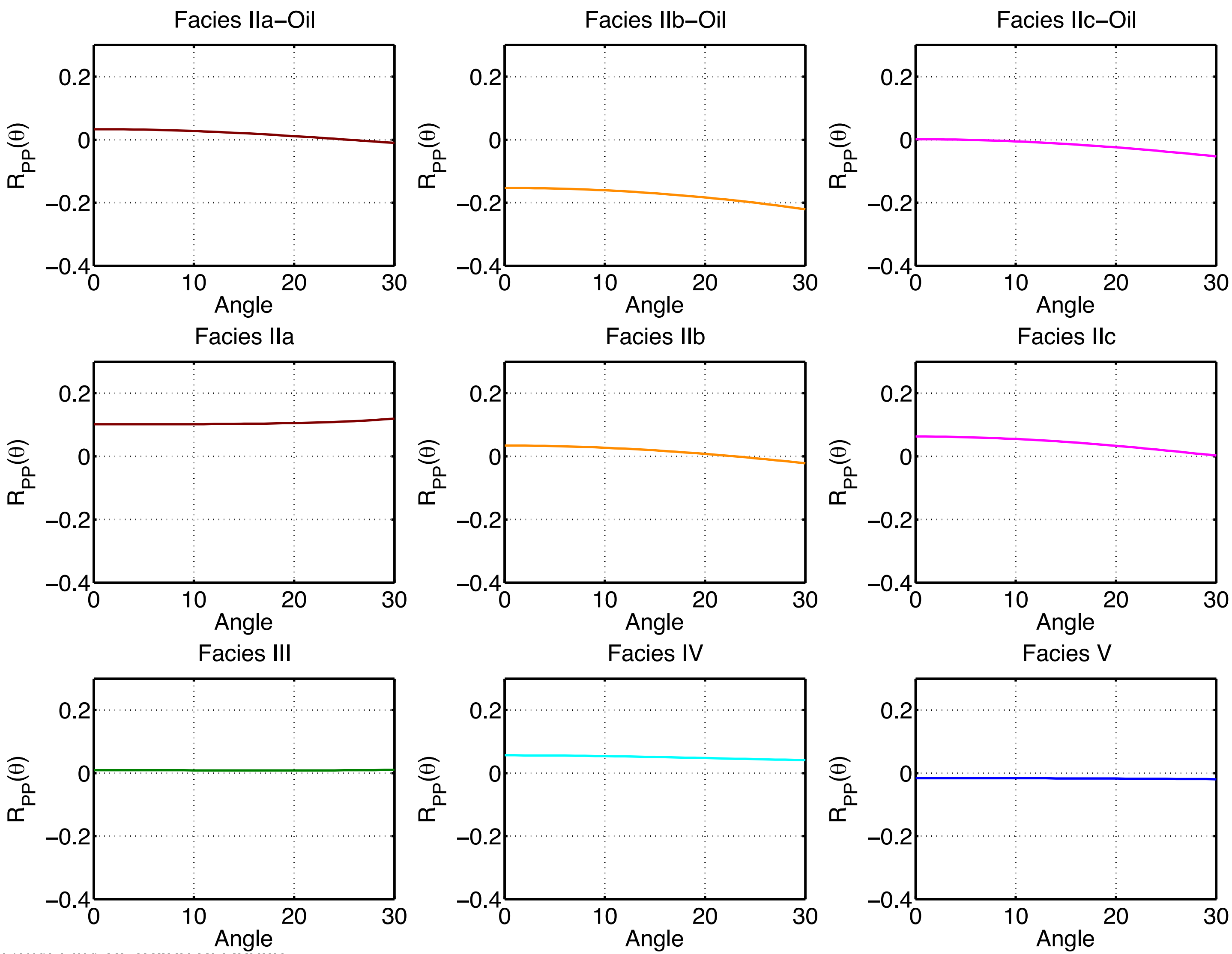

Step 4: Compute synthetic angle-dependent reflectivity for realizations of Facies IV overlying all the facies

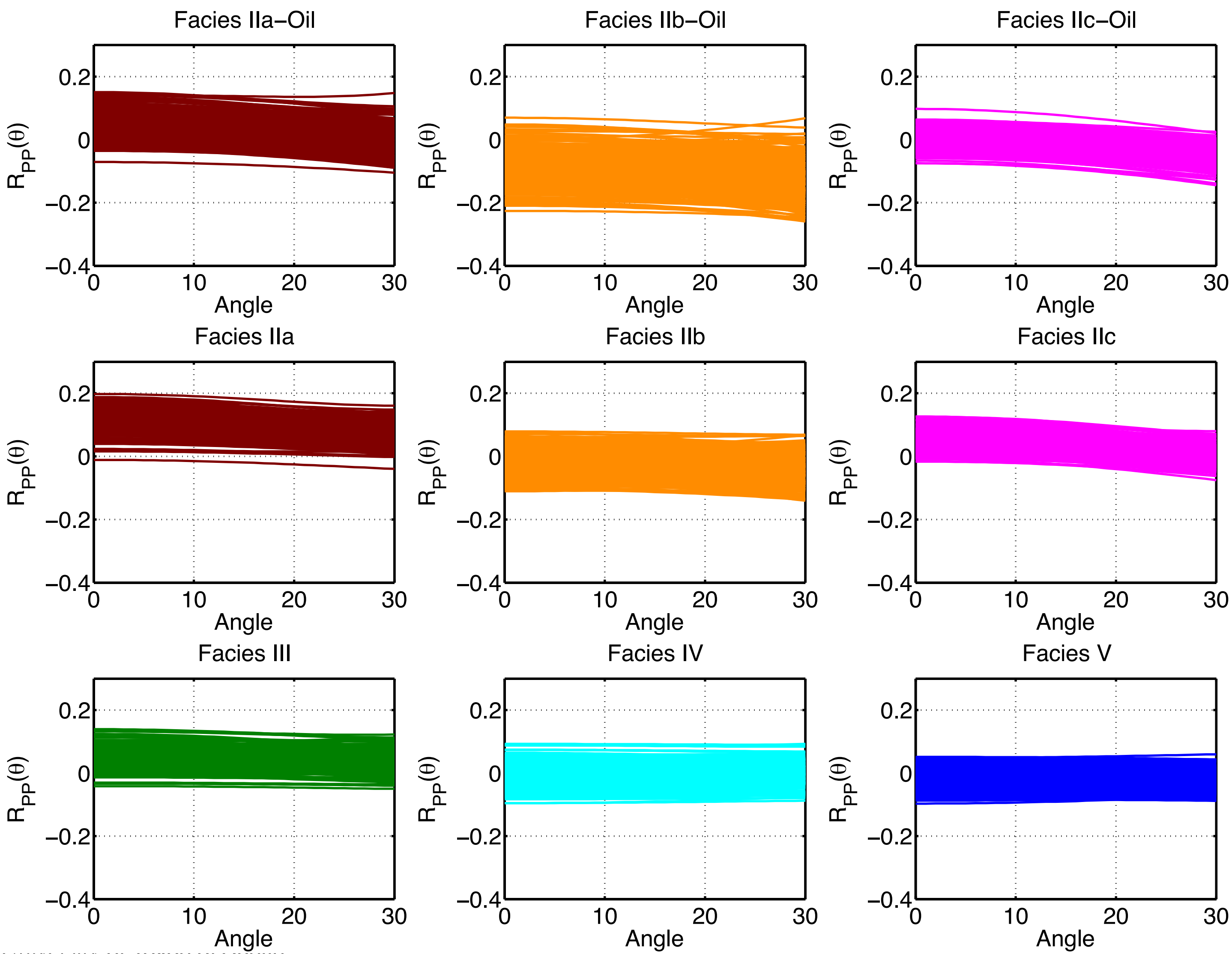

Step 5: Compute intercept and gradient for each case

Black points are the mean values

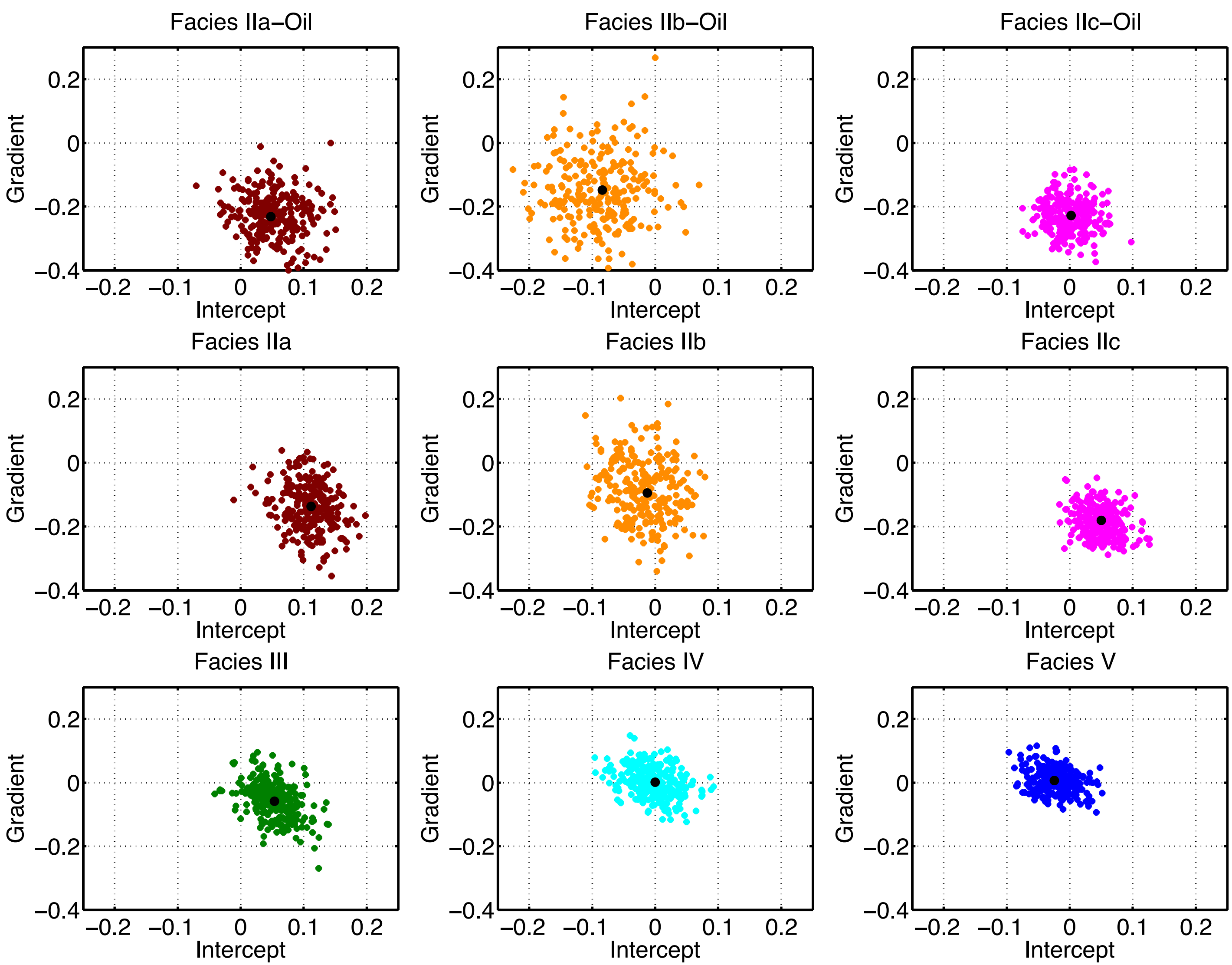

Combining all facies

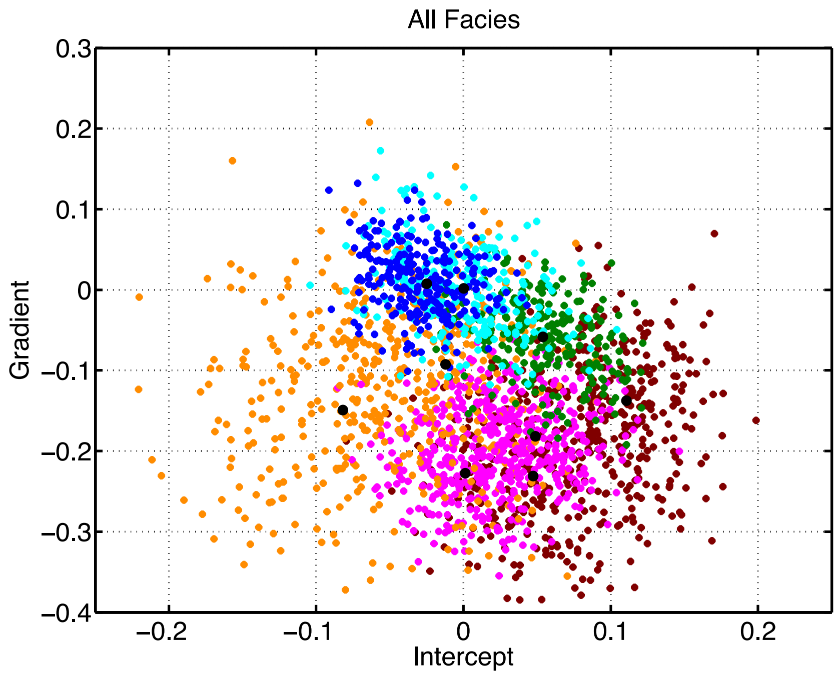

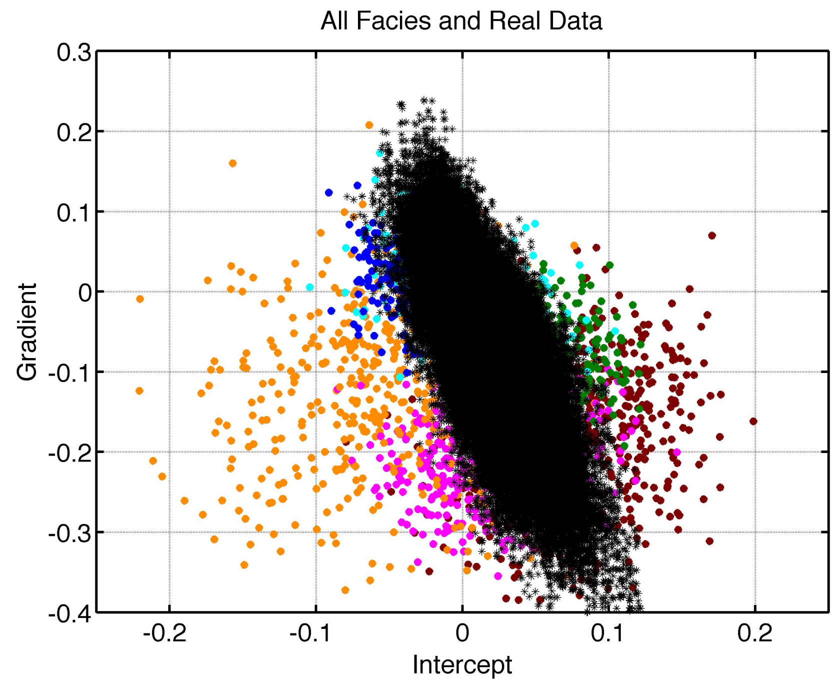

Step 6: Compute the Mahalanobis distance for each real data point

$$D^2 = (\mathbf{x} - \mu_i)^T \Sigma^{-1} (\mathbf{x} - \mu_i)$$

$\mathbf{x}$ = Measurement

μ_i = vectors for the measurement means for different classes

Σ = covariance of the training data

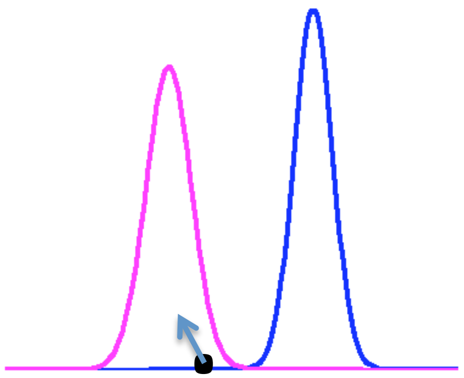

This is essentially linear discriminant analysis.

We have 9 different classes, or training data, so there are nine elements in the mean vector. The covariance matrix corresponds to the covariance of the Intercept and Gradient for each class.

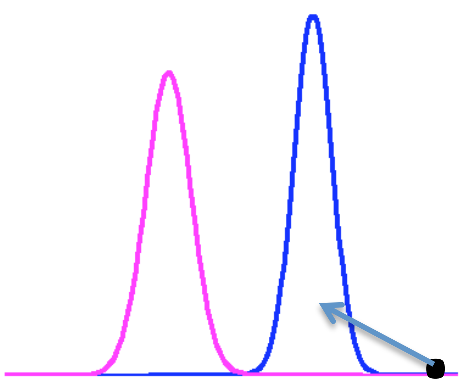

We compute the D^2 value between each measurement and each class.

The D^2 is the distance between the measurement and the mean of the training data sets.

The measurement is assigned the most likely class where D^2 is minimum.

Step 6: Compute the Mahalanobis distance for each real data point

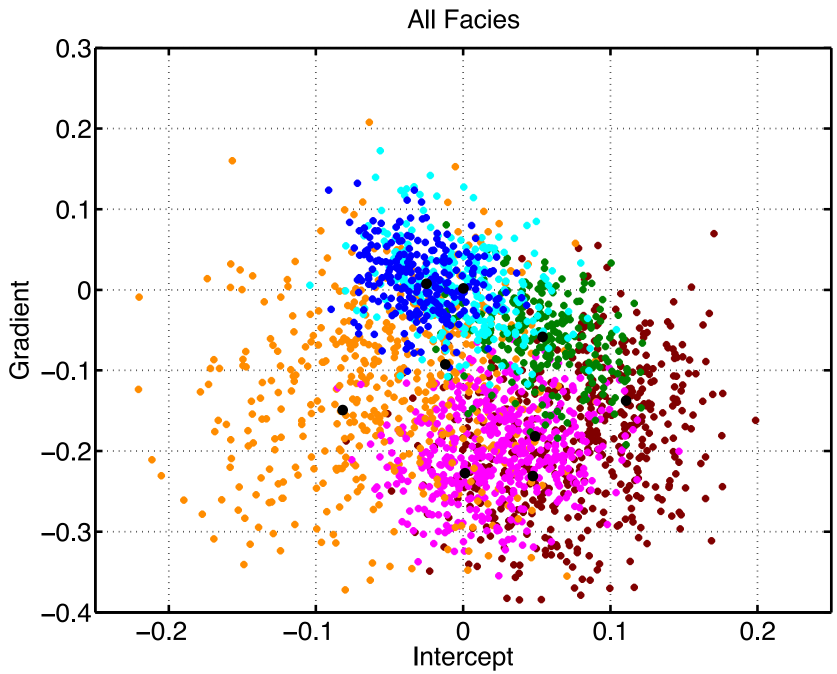

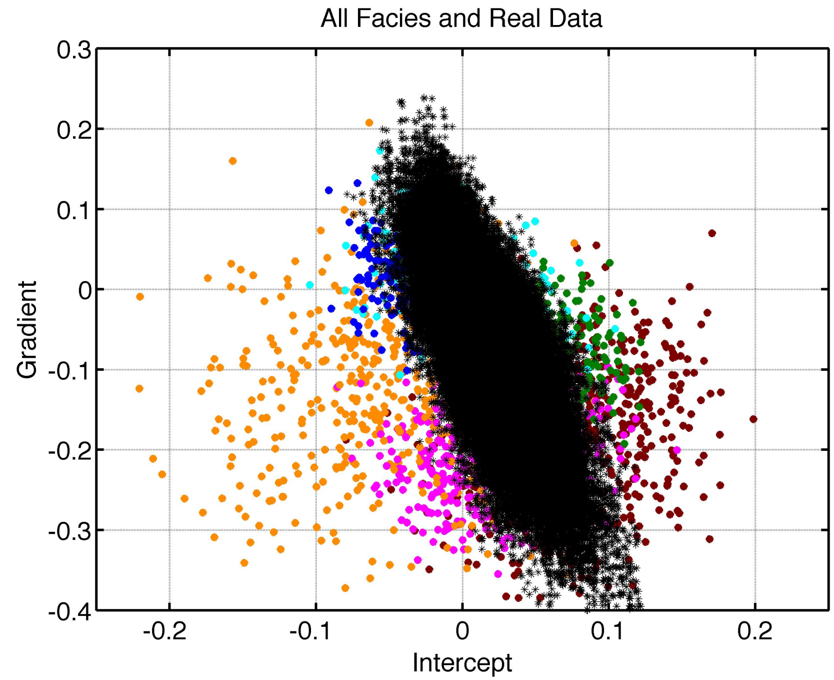

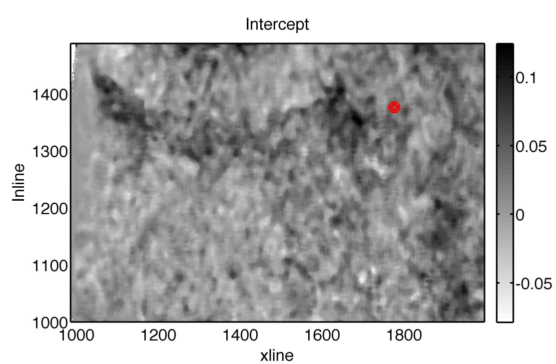

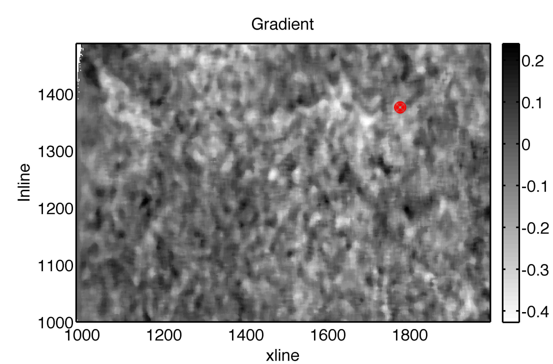

Step 6: Compute the Mahalanobis distance for each real point

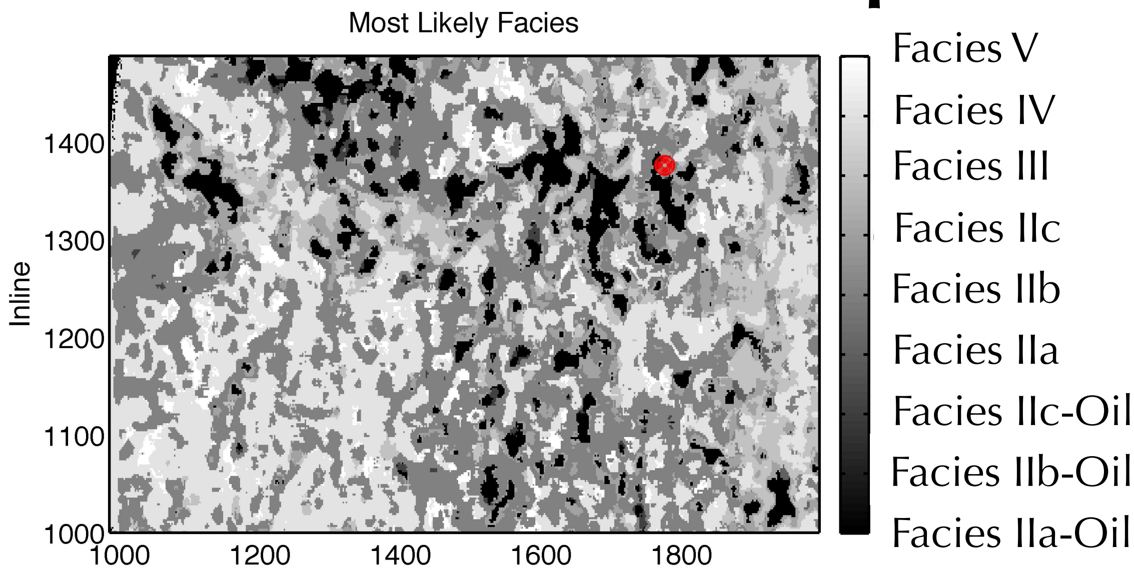

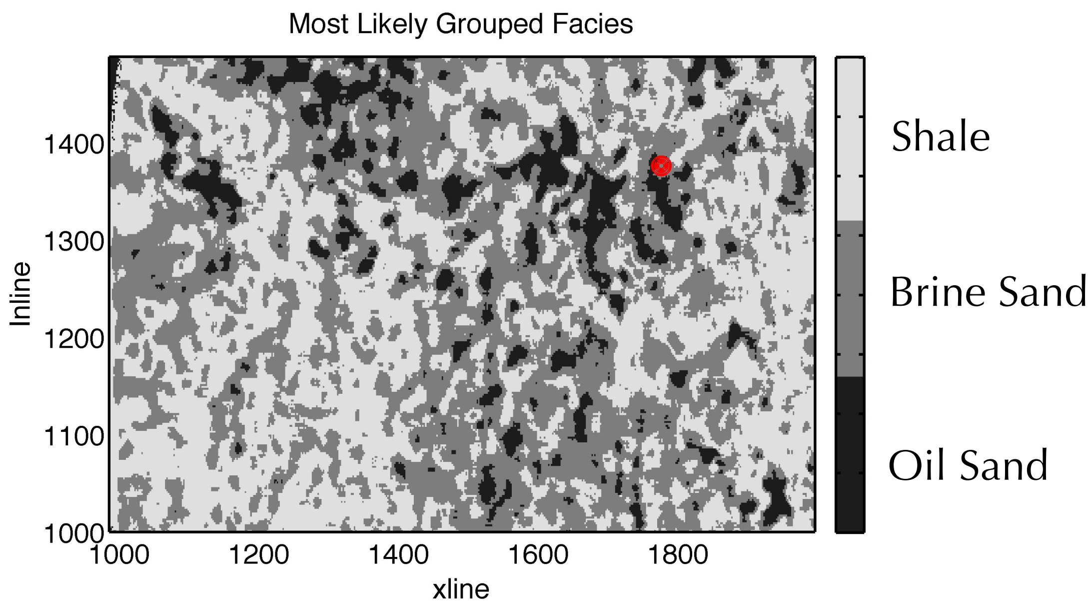

What can alter this result?

Number of simulations

Range of incidence angles

Calculation of angle-dependent reflectivity (full Zoeppritz versus and approx.

Mean and standard deviation of CDFs (or PDFs) for each of the classes

References

Aki, K., and Richards, P, 1980, Quantitative seismology theory and methods, Freeman.

Avseth, P., T. Mukerji, and G. Mavko, 2005, Quantitative Seismic Interpretation: Cambridge Press.

Fatti, J.L., Smith, G.C., Vail, P.J., Strauss, P.J., Levitt, P.R., 1994, Detection of gas in sandstone reservoirs using AVO analysis: Geophysics, 59, 1362-1376.

Gidlow, P.M., Smith, G.C., and Vail, P.J., 1992, Hydrocarbon detection using fluid factor traces, a case study: How useful is AVO analysis? : Joint SEG/EAEG summer research workshop, Technical Program and Abstracts, 78-79

Shuey, R. T., 1985, A simplification of the Zoeppritz equations: Geophysics, 50, 609–614.

Wiggins, R., Kenny, G. S., S., G., and McClure, C. D., 1983, A method for determining and displaying the shear-velocity reflectivities of a geologic formation: European Patent Application 0113944.

Zoeppritz, K., 1919, Erdbebenwellen VIIIB, Ueber Reflexion and Durchgang seismischer Wellen durch Unstetigkeitsflaechen: Goettinger Nachrichten, I, 66-84.